Arabian Journal of Chemistry (2022) **15**, 103841

King Saud University

Arabian Journal of Chemistry

www.ksu.edu.sa
www.sciencedirect.com

ORIGINAL ARTICLE

L-Glutamic acid loaded collagen chitosan composite scaffold as regenerative medicine for the accelerated healing of diabetic wounds

Bharat Kumar Reddy Sanapalli [a], Rishita Tyagi [a], Afzal B. Shaik [b], Ranakishor Pelluri [c], Richie R. Bhandare [d,f,*], Sivakumar Annadurai [e,*], Veera Venkata Satyanarayana Reddy Karri [a,*]

[a] *Department of Pharmaceutics, JSS College of Pharmacy, JSS Academy of Higher Education & Research, Ooty, Nilgiris, Tamilnadu 643001, India*
[b] *Department of Pharmaceutical Chemistry, Vignan Pharmacy College, Vadlamudi-522213, Andhra Pradesh, India*
[c] *Department of Pharmacy Practice, Vignan Pharmacy College, Vadlamudi-522213, Andhra Pradesh, India*
[d] *Department of Pharmaceutical Sciences, College of Pharmacy & Health Sciences, Ajman University, Ajman, United Arab Emirates*
[e] *Department of Pharmacognosy, College of Pharmacy, King Khalid University, Abha-61421, Saudi Arabia*
[f] *Center of Medical and Bio-Allied Health Sciences Research, Ajman University, Ajman P.O. Box 346, United Arab Emirates*

Received 8 January 2022; accepted 13 March 2022
Available online 16 March 2022

KEYWORDS

Diabetic wound;
L-Glutamic acid;
Collagen;
Chitosan;
Scaffold

Abstract Diabetic wounds (DWs) are characterized by prolonged inflammation, which poses a significant challenge for clinicians and researchers to promote healing. In this study, we fabricate L-Glutamic acid (LGA) loaded collagen/chitosan (COL-CS) composite scaffold for the accelerated healing of DW. The characterization outcomes of the composite scaffold revealed that a crosslinked scaffold holds optimum porosity, low matrix degradation, and sustained drug release in contrast to a non-crosslinked scaffold. *In vitro*, LGA composite scaffolds have not exhibited any toxicity on 3T3L1 cell lines. *In vivo*, the LGA composite scaffold has shown significantly ($p < 0.001$), higher rates of wound contraction than those in control and COL-CS scaffold treated groups. In addition, MMP-9 levels were also significantly reduced in LGA composite scaffold-treated group compared with those in the control and COL-CS scaffold treated group. Thus, the LGA composite scaffold

* Corresponding authors at: Department of Pharmaceutics, JSS College of Pharmacy, JSS Academy of Higher Education & Research, Ooty, Nilgiris, Tamil Nadu-643001, India (VVSR Karri). College of Pharmacy & Health Sciences, Ajman University, PO Box 340, Ajman, United Arab Emirates (R.R. Bhandare). College of Pharmacy, King Khalid University, Abha 61421, Saudi Arabia (SK Annadurai).
E-mail addresses: bharathsanapalli@yahoo.in (B. Kumar Reddy Sanapalli), narayana.reddy@jssuni.edu.in (R. Tyagi), bashafoye@gmail.com (A.B. Shaik), ranampharm@gmail.com (R. Pelluri), r.bhandareh@ajman.ac.ae (R.R. Bhandare), sannadurai@kku.edu.sa (S. Annadurai), ksnreddy87@gmail.com (V. Venkata Satyanarayana Reddy Karri).
Peer review under responsibility of King Saud University.

Production and hosting by Elsevier

https://doi.org/10.1016/j.arabjc.2022.103841

may serve as a promising therapy in DW due to its unique modulatory effect on inflammatory biomarker MMP-9.

1. Introduction

Diabetes mellitus (DM) is one of the major health concerns with increased incidence globally. DM, a common endocrine disorder, results in increased blood glucose due to the absence or insufficiency of insulin production (International Diabetes Federation, 2017). Though DM is well managed in due course, it results in several complications such as neuropathy, nephropathy, vasculopathy, and immunopathy. These comorbidities increase the risk of other DM related complications. Among which diabetic wound (DW) is the most devastating complication with amputation (Lipsky et al., 2004). About 25% of patients with DM tend to get DW in their lifetime. The delayed healing of DW is due to prolonged inflammation and diminished growth factors, which eventually leads to extracellular matrix degradation. The presence of microbial infections further worsens this condition. When left untreated, these wounds may develop into gangrenes prompting the removal of organs (International Diabetes Federation, 2017; Lipsky et al., 2004).

Although several standard care treatments such as patient education, controlling blood sugar, wound debridement, pressure offloading shoes, surgeries, and advanced dressings are available, most of them haven't addressed all the prerequisites because of the multifactorial pathophysiology of DW and cost associated with the treatments (Alexiadou and Doupis, 2012; Frykberg and Banks, 2015). As mentioned above, continuous inflammation with inappropriate tissue management is the major reason for impaired healing (Mat Saad et al., 2013). Increased levels of proinflammatory and inflammatory mediators in DW are the critical etiological factors responsible for the chronic inflammatory condition resulting in decreased growth factors (Falanga, 2005). Improper matrix formation is due to the rapid degradation of formed extracellular matrix because of increased matrix metalloproteinases (MMPs). In the family of MMP, MMP-2, and MMP-9 are the major MMPs responsible for chronic inflammation (Caley et al., 2015). Literature also suggests a rapid increase in the levels of MMP-9 as compared to those of MMP-1, 2, and 8 in the chronic wound fluid. Inhibition of the MMP-9 is reported to lead to efficient healing of wounds in diabetic conditions. Local treatment with the agent that blocks elevated inflammatory mediators (MMP-9) can restore cutaneous homeostasis and matrix formation and lead to better wound healing (Gill and Parks, 2008; Reiss et al., 2010).

L-Glutamic acid (LGA), a gamma-aminobutyric acid (GABA) precursor, was used as a drug candidate to suppress the elevated levels of MMP-9, which may be the reason for the prolonged inflammatory phase (Wu et al., 2017; Huang et al., 2011). Apart from the drug candidate, wound dressing also plays a major role in enhanced recovery as it provides the most optimum conditions for DW healing while protecting the wound from infection.

Although many wound dressings have been prepared, DW management is still in its infancy (Bano et al., 2017). This may be due to the inability of the dressings to satisfy all the necessary prerequisites (Zhang et al., 2015; Foroumadi et al., 2001; Deutsch et al., 2017; O'Meara et al., 2000). The ideal properties of a wound dressing include preserving the moist environment, interfacial wound electrolyte balance for the exchange of gases, and removal of excess exudates besides the necessity to promote accelerated wound healing (Jayakumar et al., 2011; Xiao et al., 2011). Further, it should be readily available, cost-effective, and non-allergic, providing hemostatic property (Bano et al., 2017).

In this context, three-dimensional bioengineered substituents such as scaffolds, nanofibers, films, microfibers, and hydrogel have gained more attention because of their multifaceted effects (Nair and Laurencin, 2005; Ulery et al., 2011). Among the bioengineered substituents, the scaffold has gained significant interest due to their desirable characteristics like tissue biocompatibility, preservation of the moist environment, the large surface area for absorbability of tissue exudates, and interconnecting pores for high oxygen supply to facilitate optimal tissue regeneration (Vinatier et al., 2009; Morrison, 2009). Moreover, the use of two or more polymers in combination may tailor the desirable characteristics to the scaffold (Gautam et al., 2013; Jafari et al., 2017).

Collagen (COL) is the most abundant structural protein that plays an essential role in maintaining the biological and structural integrity of ECM and also aids in mechanical support to tissues (Ricard-Blum, 2011). In recent years, investigation on COL-based studies has gained significant interest in tissue engineering technology (Inzana et al., 2014; Lu et al., 2015; Ghazanfari et al., 2015; Meimandi-Parizi et al., 2013). Physically, COL is well organized and can accommodate any component/drug due to its mesh/network-like structural nature. Pharmaceutically, COL offers porous structure to the scaffold, biocompatibility, bio-absorbability, and permeability (Gelse et al., 2003; Chevallay and Herbage, 2000; Wolf et al., 2009). These essential properties aid in achieving the controlled release of the drug. In addition, COL possesses specific pharmacological functions like morphology regulation, bio-adhesion, cell migration and cell differentiation (Wang et al., 2015; Takitoh et al., 2015; Maslennikova et al., 2015). Despite these excellent biomedical properties, it exhibits poor structural and mechanical ability. So, to circumvent these limitations, many crosslinking strategies have been put-forth by physical or chemical treatment (Gordon and Hahn, 2010).

Chitosan (CS) is a natural polymer, structurally homologous to glycosaminoglycan, and found to be biocompatible and bioabsorbable (Balan and Verestiuc, 2014). In recent years, CS-based studies have been drastically increased in biomedical fields due to its massive role in wound healing, dermal regeneration, and stimulation of growth factors along with its antimicrobial properties (Ueno et al., 2001; Patrulea et al., 2015; Dragostin et al., 2016). In addition, CS is capable of forming a porous scaffold with large number of interconnected pores up on freeze drying (He et al., 2011).

The porous nature of the scaffold enhances liquid absorption and facilitates the exchange of essential gases upon topical application (Anisha et al., 2013; Dutta et al., 2011). Moreover, CS exhibits few practical disadvantages like brittleness and lack of ability to control drug release from the encapsulated dosage form. However, several studies have reported that the blending of CS with other biopolymeric materials overwhelms these limitations (Ammar et al., 2009; Kamel, 2013; Kamel and Abbas, 2018). Several reports have stated that the blending of CS with COL has increased the thermal stability, mechanical strength, and scaffold biodegradation (Ureña-Saborio et al., 2018). Thus, LGA-loaded collagen (COL) and chitosan (CS) composite scaffolds were formulated to suppress the prolonged inflammatory phase and promote accelerated DW healing.

2. Materials and methods

2.1. Reagents and cell line

- L-Glutamic acid (Sigma chemicals Co. Ltd, Mumbai, India)
- Chitosan low molecular weight (Sisco Research Laboratories Pvt. Ltd., Mumbai, India)

- Type-1 collagen from rat tail (Sigma chemicals Co. Ltd, Mumbai, India)
- Glacial acetic acid (Merck Millipore, Mumbai, India)
- Ethanol (Merck Millipore, Mumbai, India)
- 1-ethyl-(Alexiadou and Doupis, 2012) carbodiimide hydrochloride (EDC) (Merck Millipore, Mumbai, India)
- N-hydroxy succinimide (NHS) (Merck Millipore, Mumbai, India)
- 2-(N-morpholino) ethane sulfonic acid (MES) (Merck Millipore, Mumbai, India)
- Sodium dihydrogen orthophosphate (NaH_2PO_4) (Qualigen Fine Chemicals, Mumbai, India)
- Sodium hydroxide (NaOH) pellets (Qualigen fine chemicals, Mumbai, India)
- 3-(Frykberg and Banks, 2015) −2, 5-diphenyl tetrazolium bromide (MTT) (Thermo Fisher, Mumbai, India)
- Mouse embryonic fibroblast cells (3 T3-L1) (National Centre for Cell Sciences, Pune, India).
- Mueller Hinton broth (MHB) (Himedia Labs, Mumbai, India)
- Dimethyl sulfoxide (DMSO) (Himedia Labs, Mumbai, India)
- D-Glucose (Merck Millipore, Mumbai, India)
- Ehrlich's reagent (Himedia Labs, Mumbai, India)

2.2. Preparation of LGA composite scaffold

CS solution (3% w/v) and COL solution (1% w/v) were prepared in 0.75 M acetic acid solution. The pH of the COL solution was adjusted to 7.2 by adding 2 M NaOH at 4 °C. The LGA (1% w/w) dispersion was added to the cold COL solution to achieve the LGA-COL solution. Later, the obtained LGA-COL solution was added to the CS solution to obtain LGA composite mixture. The mixture was stirred overnight to achieve uniform homogeneity. The entrapped bubbles in the mixture were removed by bath sonicator (Bandelin RK 100H, Germany) for 10 min. Then this mixture was poured in petri-dishes and kept in the deep freezer at −60°C (Labline) for 12 h, followed by lyophilization (Christ Alpha 1–2) at −60°C for 72 h to obtain the LGA composite-scaffolds (Natarajan et al., 2019). The same method was used to prepare the placebo (without LGA).

2.3. Crosslinking of LGA composite scaffold

MES (0.488 g) was suspended in 50 mL of millipore water to obtain a solution of pH 5.6. Further, prepared LGA composite scaffolds (50 mg) were soaked in 20 mL of MES buffer for 30 min. Meanwhile, the buffer mixture was prepared in another beaker using 19.5 mL of MES solution, 0.014 g of NHS, and 0.1264 g of EDC. For crosslinking, the soaked scaffold was dipped in the buffer mixture for 4 h. The crosslinked scaffold was sieved out and washed twice after keeping in contact with 0.1 M sodium dihydrogen orthophosphate, 1 M NaCl, and 2 M NaCl for about 2 h and 24 h, respectively (Karri et al., 2016; Powell and Boyce, 2006). Further evaluation was performed for the prepared scaffolds. The same method was used to crosslink the placebo (without LGA).

2.4. Scaffold characterization

2.4.1. Porosity

Liquid displacement is the method used widely to determine the scaffold's porosity. Ethanol was used as a displacement liquid as it meets all the characteristics of an ideal solvent like effortless penetration, no contraction, or swelling of the scaffolds (Karri et al., 2016). The porosity of scaffolds was calculated using the formulae.

$$Porosity(\%) = \frac{Ww - Wd}{SV} X100$$

Where W_w and W_d are the wet and initial dry weights of the scaffolds, respectively while SV is the volume of scaffold.

2.4.2. Swelling test

Weight of dry scaffolds were determined prior to the start of the analysis. Further incubation of the weighed scaffolds was done using phosphate-buffered saline (PBS) at pH 7.4 in a humidified atmosphere of 5% CO_2 for 1, 12, 24, 36, 48, 60 and 72 h at 37 °C. The excess PBS was removed by blotting with filter paper and the weight was measured (Baheiraei et al., 2018). The swelling ratio of crosslinked and non-crosslinked composite scaffolds was calculated using the formulae.

$$Wab = \frac{[Ww - Wd]}{Wd} \times 100$$

Where Wab is the water adsorption percentage at equilibrium. Wd and Ww are the dry and wet weights of the scaffolds, respectively.

2.4.3. Matrix degradation

Crosslinked and non-crosslinked LGA composite scaffolds (1x1cm) were incubated in PBS of pH 7.4 with 10,000 μ/mL of lysozymes for 7 days at 37°C. These scaffolds were then washed with millipore water to remove ions adhered on the surface and subjected to lyophilization. Wi and Wf are the initial weight and weight after freeze-drying of the scaffolds, respectively (Kim and Kim, 2013). The degradation rate was calculated using the formulae.

$$\%Degradation = \frac{[Wi - Wf]}{Wi} \times 100$$

2.4.4. Scanning electron microscopy analysis for morphological studies

The cross-sectional structural morphology of the prepared composite scaffolds was determined using field emission scanning electron microscopy (FE-SEM, Hitachi S-4800). The samples (5 × 5 mm) were subjected to coating with a thin film of gold and positioned on adhesive stub using 10 kV of operational voltage. Randomized selection of fifty pores was taken place to determine pore size, and three scaffolds with three different cross-sections from each group were chosen to determine pore size (Karri et al., 2016).

2.4.5. In vitro release of LGA from composite scaffold

The crosslinked and non-crosslinked LGA composite scaffolds (3 × 3 cm) were immersed in 20 mL PBS of pH 7.4 at 37°C.

The supernatant was collected periodically and replaced with an equivalent amount of PBS. For further analysis, filtration of samples was performed using 0.2μ membrane filter (Karri et al., 2016). The drug release was determined by using LGA standard curve developed with Liquid Chromatography-Mass Spectrophotometer (LCMS 8030, Shimadzu).

2.4.6. Thermal compatibility test using differential scanning calorimetry

The thermal behavior of the crosslinked LGA composite scaffold was characterized by using differential scanning calorimetry (DSC, Q100, TA instruments, USA) in a heating rate of 10 $^{0}C\ min^{-1}$ at a temperature range of 20–250 ^{0}C. The dry nitrogen was used as a purge gas at a stream pace of 50 mL min − 1. Aluminum pan was used for recording the DSC graphs. Indium metal was utilized as a standard for the temperature alignment of the hardware.

2.5. In vitro biocompatibility studies

Biocompatibility of the crosslinked and non-crosslinked LGA composite scaffolds was assessed by MTT assay. Scaffolds were sterilized (15mmdiameter) in 75% ethanol for 30 min, later washed with millipore water for 5 min. The scaffold was placed in each well containing with 2 mL of Dulbecco's modified Eagle's medium, and later 3 T3-L1 cells were added. The study was performed for 72 h, wherein both control and test solutions were used for proper comparison (Karri et al., 2016).

2.6. Antibacterial evaluation

Minimum inhibitory concentration (MIC) of LGA composite scaffold was determined by the Micro-broth dilution method using MHB. *Staphylococcus aureus* (*S. aureus*; NCIM 5022), *Pseudomonas aeruginosa* (*P. aeruginosa*; NCIM 2036), *Escherichia coli* (*E. coli*; NCIM 2567) and *Klebsiella pneumonia* (*K. pneumonia*; NCIM 2706) bacterial strains were diluted at a ratio of 1:1000 MHB to obtain turbidity of 0.5 McFarland. Further, the bacterial cultures were hyperglycated using D-glucose (800 mg/dL) (Xie et al., 2017; Geerlings et al., 1999). LGA composite scaffold was crushed and dissolved in DMSO, the obtained solution was used as a test sample. This study used ciprofloxacin, a broad-spectrum antibiotic as positive control and sterile DMSO as a negative control. In each well of 96 plate, 100 μL of hyperglycated bacterial suspension and 50 μL of LGA composite scaffold extract were added followed by serial dilution. The plates were incubated at 37 °C for 20–24 h, whereas, for *P. aeruginosa*, the incubation was performed for 24–28 h at 37 °C. The absorbance was recorded at a wavelength of 600 nm in Tecan-i-control, 1.7.1.12 (Eloff, 1998).

2.7. In vivo wound healing study

Adult Wistar albino rats of either sex weighing around 180–200 g were used for the study. Intraperitoneal injection of 30 mg/kg streptozotocin in 0.1 M cold citrate buffer of pH 4.5 and high fat diet was used to induce diabetes. Rats with ≥ 250 mg/dL of blood glucose were separated and monitored for 7 more days. The rats that continually showed increased levels of blood glucose were considered for the study (Zhang et al., 2009).

An open wound (2 × 2 cm^2 with a depth of 2 mm) was created on the dorsal region of the diabetic rat under anesthetic conditions (Ketamine: Xylazine 100:15 mg/kg). The Institutional Animal Ethical Committee of JSS College of Pharmacy, Ooty, approved all the animal studies with protocol number JSSCP/OT/M.Pharm/21/2018–19.

The animals were segregated into three groups (n = 6) and housed individually after the anesthetic recovery. Wounds in group 1 were covered with sterile gauze (control), group 2, and group 3 animals were treated with composite scaffold (Crosslinked scaffold without LGA) and LGA composite scaffold (Crosslinked scaffold with LGA), respectively throughout the study duration (Sanapalli et al., 2018).

2.8. Assessment of wound contraction

The healing wound (Caley et al., 2015) area was measured by tracing the borderline of unhealed wound on an overhead projector sheet (OHP). Graph paper was used to calculate the area (Natarajan et al., 2019). Percentage wound contraction was calculated using the formula.

$$\%\ wound\ contraction\ = \frac{wound\ area\ on\ day\ 0\ -\ wound\ area\ on\ a\ particular\ day}{wound\ area\ on\ day\ 0} \times 100$$

2.9. Hydroxyproline estimation

Granulation tissue excised on days 7, 14, and 21, were subjected to autoclaving for acid hydrolysis (6 M HCl) at 120 °C for 20 min. 450 μL of Chloramine-T was added to the hydroxylate, mixed softly, and left for 25 min at room temperature to undergo oxidation. To the oxidized mixture, 500 μL of Ehrlich's reagent (p-dimethyl amino benzaldehyde in perchloric acid/n-propanol) was added and incubated at 65 °C for 20 min. The absorbance of the obtained complex was measured at the wavelength of 550 nm. Hydroxyproline concentration in the tissue was expressed as μg/mg (Reddy and Enwemeka, 1996).

2.10. Histopathological studies

Wound tissues were excised on days 7, 14 & 21 and stored in formalin solution (10%) prepared in millipore water. Tissues were sectioned into a thickness of 6 μm using a microtome (Model No: RM2135, Leica, U.K). Sections were mounted on a glass slide and Hematoxylin and eosin (H&E) were used for staining. All microscopical examinations were performed under 40x magnification using a motic microscope (Model No: MLX-i Plus, Magnus, India) (Sanapalli et al., 2018).

2.11. ELISA test

MMP-9 estimation using ELISA kit (R&D Systems) was done according to the directions provided by the manufacturer. Tis-

sue samples isolated from the wound area were minced using tissue homogenizer and the homogenate was subjected to centrifugation. The supernatant was collected and diluted 100-folds by means of assay buffer. The concentration of MMP-9 in the samples obtained from all the groups (control, composite scaffold and LGA composite scaffold) were estimated on day 7, 14 and 21.

2.12. Statistical analysis

The findings are expressed in the form of Mean ± SD. Statistical analysis was carried out using the V6.01 Graph pad prism (San Diego, CA, USA). Statistical significance was carried out using One Way Analysis of Variance followed by Dunnet's posthoc study. Values with $p \leq 0.05$ are considered to be significant.

3. Results and discussion

3.1. Physical examination of LGA composite scaffold

On examination, the composite scaffolds were found to be off-white in color. Further inspection of the scaffold revealed that all of them had cohesive property with high integrity which increases the mechanical stability and flexibility of the scaffold.

3.1.1. Porosity studies

The findings related to the porosity of non-crosslinked and crosslinked LGA composite scaffolds are given in Table 1. The porosity of non-crosslinked LGA composite scaffolds was found to be higher in comparison with that of crosslinked LGA composite scaffolds. The scaffold's porosity is anticipated to assist in the transfer of nutrients, absorption of metabolic waste, cell binding, proliferation, and migration, which are essential characteristics of tissue regeneration (Jayakumar et al., 2011). However, high porosity leads to the reduced mechanical strength of the scaffold. The probable reason for the decrease of porosity after crosslinking may be because of interactions between carboxyl group of COL with amino (>C = O---NH; amide bond) and hydroxyl (>C = O---OH; ester bond) group of CS in the presence of EDC/NHS crosslinkers (Wang et al., 2003; Kołodziejska et al., 2006). Thus, cross linking helps out in upholding the mechanical strength of the LGA composite scaffolds. The obtained results correlate with (Mane et al., 2015) (Mane et al., 2015).

3.1.2. Swelling test

The findings associated with swelling of non-crosslinked and crosslinked LGA composite scaffolds are given in Table 1. The percentage of PBS absorption was found to be more in the non-crosslinked LGA composite scaffold than in the cross-linked LGA composite scaffold. The water absorption property of the non-crosslinked scaffold is attributed to the hydrophilicity of both COL and CS. This property is mainly responsible for maintaining the 3D shape and structure of the scaffold (Ma et al., 2003; Rehakova et al., 1996). However, higher water absorption might cause swelling of the scaffold, leaving it in a deformed shape, affecting cell division and proliferation (Mane et al., 2015). The concentration of CS and crosslinking play a major role in water absorption. In the present study, we found that the water absorption capacity gradually diminished by the increased concentration of CS. Increased mechanical strength of the scaffold is attributed to crosslinking, which aids in maintaining the physical structure and shape without affecting the development of the cell. In general, the swelling ratio is inversely proportional to the degree of crosslinking. As crosslinking degree increases, the swelling ratio decreases because of decreased hydrophilic groups due to crosslinking (Rehakova et al., 1996). These results were in good agreement with the studies by (Karri et al., 2016; Karri et al., 2016).

3.1.3. Matrix degradation studies

The non-crosslinked LGA composite scaffold has shown a rapid degradation rate after post-incubation with the PBS of pH 7.4 containing lysozymes on the first day and continued the same rate of degradation for the next six days. Contradic-

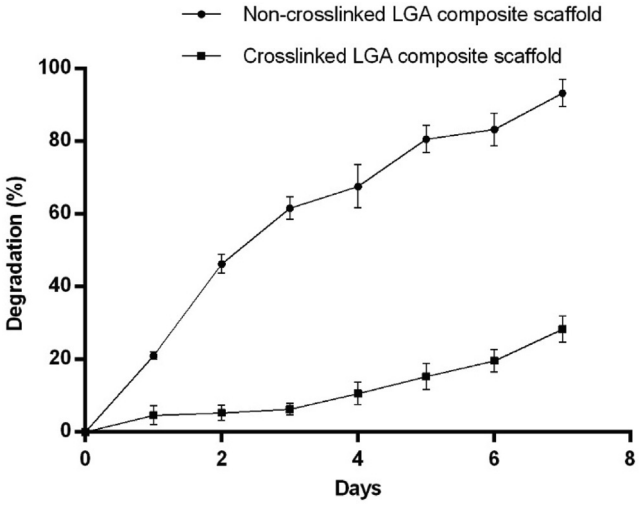

Fig. 1 Matrix degradation of LGA composite non-crosslinked and crosslinked scaffolds from day 1 to 7 in phosphate buffer pH 7.4 at 37^{0}C, showing non-crosslinked scaffold degraded progressively for seven days. Contrary to this, the crosslinked scaffold degradation rate decreased greatly, indicating enhanced resistance to the enzymatic degradation.

Table 1 Percentage porosity and water absorption properties of non-crosslinked and crosslinked LGA composite scaffold.

S. No	Scaffold type	% of porosity	% of water absorption						
			1 h	12 h	24 h	36 h	48 h	60 h	72 h
1	Non-crosslinked LGA composite scaffold	93.36 ± 1.98	7.2	16.4	27.6	35.9	49.1	58.7	74.2
2	Crosslinked LGA composite scaffold	78.54 ± 2.35	2.9	6.8	10.5	17.3	26.5	35.7	43.8

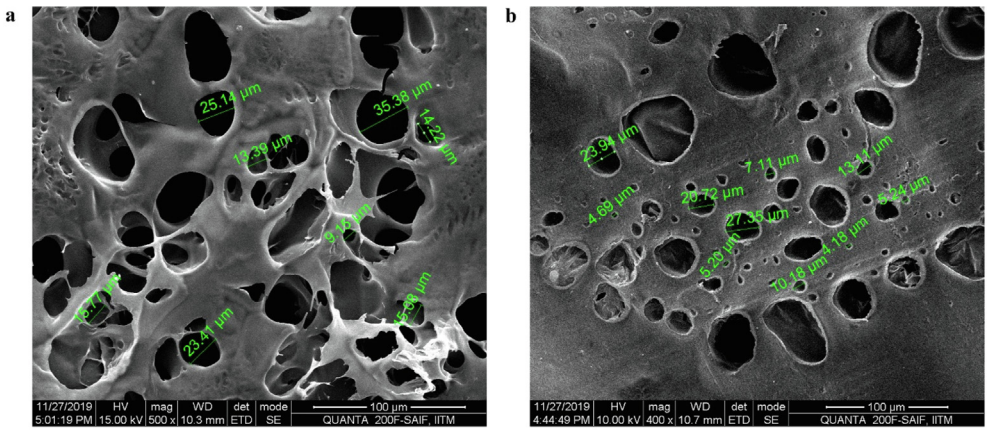

Fig. 2 Morphology of LGA loaded col-cs scaffold a) before and b) after crosslinking determination by SEM at a scale range of 100 µm showing an average pore size of 21.207 before and 12.17 after crosslinking.

tory to this, the crosslinked LGA composite scaffold has shown a delay in degradation rate (Fig. 1).

The degradation rate of the scaffold plays a major role in wound healing. In the present study, the scaffolds were designed so that it was absorbable & degradable to match up to the speed of newly formed tissue. Crosslinking leads to increased network strength and mechanical properties (Haugh et al., 2011) that, in turn, result in decreased degradation rate representing resistance to the enzymatic deterioration (Timmer et al., 2003).

3.1.4. SEM analysis

The SEM images of the scaffolds, captured at 100 µm are shown in Fig. 2a and 2b. There were larger pores visible in the non-crosslinked scaffold (Fig. 2a), whereas, in the crosslinked scaffold, smaller pores are visible with a decrease in void space (Fig. 2b).

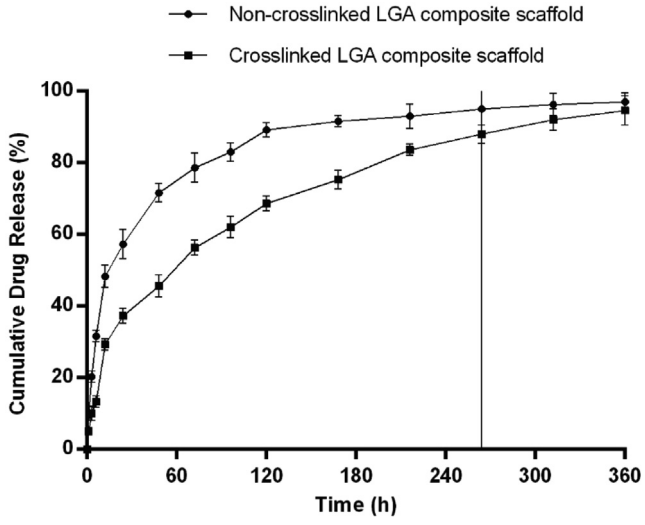

Fig. 3 *In vitro* drug release profile of LGA composite non-crosslinked and crosslinked scaffolds in phosphate buffer pH 7.4 at 37^{O}C showing a slow release of drug in all formulation followed by a sustained release and then a plateau. Data is expressed as mean ± SD (n = 3).

Crosslinking of the scaffold resulted in the decrease of void spaces due to the interlinking of the bonds. The presence of interconnected spongy arrangements emergence between composite strands was found to be prominent for cell migration, proliferation & attachment for the regeneration of tissue. An additional benefit was also observed that the porosity in the design of scaffolds was likely to contribute to enhanced permeability of O_2 to wounds (Natarajan et al., 2019; Kim and Kim, 2013).

3.1.5. In vitro LGA release studies

The release of the LGA from non-crosslinked and crosslinked composite scaffolds were performed for a period of 360 h. From the data shown in Fig. 3, a slow release of LGA in all formulations was observed, followed by a controlled release. In the initial one h, 10.33 ± 1.5% LGA was released from the LGA composite non-crosslinked scaffold, whereas only 5.0 ± 1.0% LGA was released from the LGA composite crosslinked scaffold. After six h, the LGA release from the scaffolds increased by 31.66 ± 1.52% in non-crosslinked scaffolds and 13.33 ± 1.52% in crosslinked scaffolds. After 24 h, more than 50% LGA was released from the non-crosslinked scaffold, whereas the crosslinked scaffold took 72 h to remove more than 50% of the LGA. Studies has shown a delay in the initial release of the LGA, probably because of the time taken for complete wetting of scaffold.

The crosslinked composite scaffold has shown significantly slower release than the non-crosslinked composite scaffold which may be because of the increased chemical and mechanical bonding due to crosslinking. In addition, the crosslinking property also imparts slower water absorption and swelling to the scaffold (Pillay and Fassihi, 1999). This results in the prolonged release of LGA to combat chronic inflammatory conditions in DWs. Based on the above results, crosslinked LGA composite scaffolds were selected for further evaluation and designated as LGA composite scaffold. Crosslinked scaffold without LGA is designated as a composite scaffold.

3.1.6. Thermal compatibility using DSC

Fig. 4 represents the DSC pattern of LGA, COL, CS, and LGA composite scaffold.

The characteristic transition bands illustrate the dehydration temperature of biomaterials and LGA in atmospheric

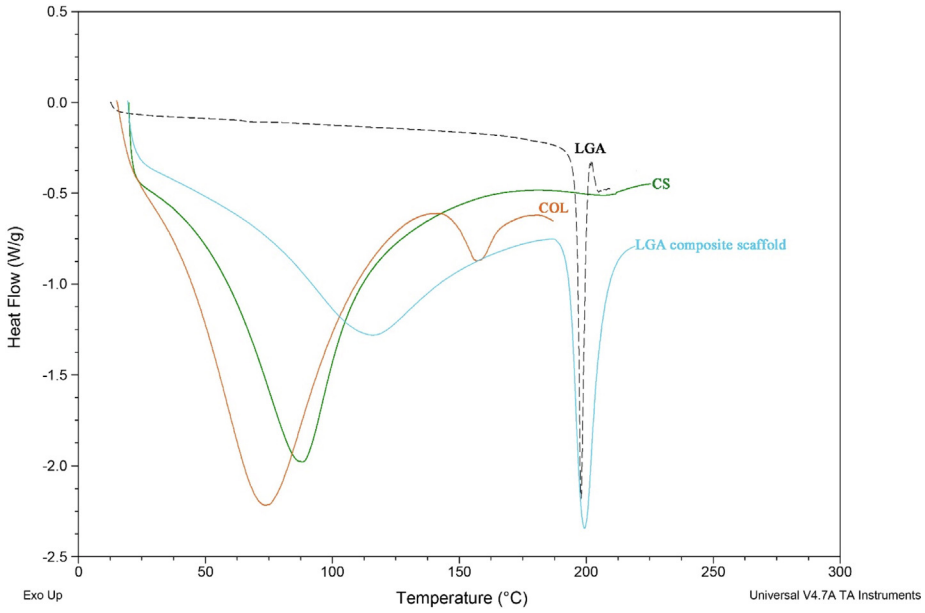

Fig. 4 DSC profile of LGA, COL, CS and LGA composite scaffold.

nitrogen. The thermogram values of LGA, COL, CS, and LGA composite scaffold were found to be 75, 90, 198, and 120 ^{0}C, respectively. These results show that the native COL is unstable at normal body temperature, which draws attention towards the crosslinking to stabilize the COL. Crosslinking of COL involves the formation of connections between fibrillar strands of COL, which inhibits its degradation by breakdown enzymes (proteases, e.g., matrix metalloproteinase). In LGA composite scaffolds, COL melting temperature has shifted to 120 ^{0}C, which indicates its stabilization by EDC/NHS crosslinking. The higher transition temperature exemplifies that LGA composite scaffold has high thermal stability than native COL.

Moreover, pure CS exhibited a transition temperature of 90 ^{0}C, while in the LGA composite scaffold the melting temperature occurred at 120 ^{0}C. However, the LGA thermogram has not exhibited any shifts in the scaffold, indicating no effect at higher temperatures. Thus, it is clear that thermodynamic properties control the durability of the composite scaffold (Sailakshmi et al., 2013).

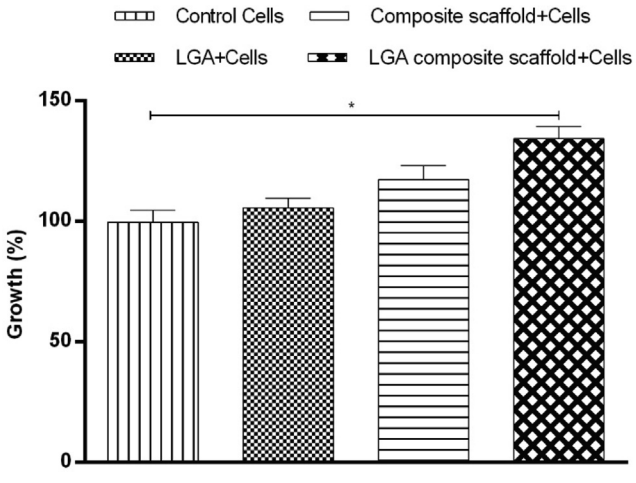

Fig. 5 Fibroblast 3 T3-L1 cells (negative control) and fibroblast cultured in the presence of LGA, composite scaffold, and LGA composite scaffolds showing percentage cell growth more in LGA composite followed by composite scaffold, LGA, and control.

3.2. In vitro cell viability studies

The results have shown that the inclusion of the LGA composite scaffold into the growth media has not stimulated any cytotoxicity towards the 3T3L1 cells. Moreover, increased cell viability was observed in the LGA composite scaffold compared to control, indicating better growth of fibroblasts in the presence of scaffolds (Fig. 5).

Fibroblasts are the key cells that mediate extracellular matrix and proteins production. They play a pivotal role in forming the structural framework required for normal wound healing. The test scaffold did not induce any cytotoxicity, and increased cell growth was found to be more in the LGA composite scaffold followed by the composite scaffold and LGA treated group compared to that of control. These results depict that uniform growth of fibroblast took place in the pores of the scaffold, indicating that the scaffolds developed were biocompatible. The increase in cell growth in the composite scaffold group is due to COL and CS as a matrix in scaffold form. Further, comparatively higher cell growth in LGA composite scaffolds might be due to COL, CS and LGA which can stimulate fibroblast differentiation. It is pertinent to add that similar results were observed from previous studies (Thangavel et al., 2017).

3.3. Antibacterial evaluation

MIC of the LGA composite scaffold was evaluated using the micro-broth dilution technique by following standard protocol. The antibacterial screening was performed against selected strains of bacteria such as *S. aureus*, *P. aeruginosa*, *E. coli* and *K. pneumonia* at a concentration in the range of 2 to 256 μg/mL. The LGA composite scaffold extract exhibited promising activity against *S. aureus* at a 2 μg/mL MIC. The extract has

Table 2 MIC of LGA composite scaffold against a selected panel of bacteria.

S. No	Samples	*S. aureus*	*E. coli*	*K. pneumonia*	*P. aeruginosa*
1	LGA composite scaffold (μg/mL)	2	< 4	6	6
2	Ciprofloxacin (μg/mL)	< 2	< 2	< 2	< 2

Note: Staphylococcus aureus (*S. aureus*); Escherichia coli (*E. coli*); Klebsiella pneumonia (*K. pneumonia*); Pseudomonas *aeruginosa* (*P. aeruginosa*).
The obtained results show that the LGA composite scaffold can reduce the pathogenic overload and pointedly improve the clinical outcome of DW patients with mild to chronic infections.

shown variable effects against *E. coli, K. pneumonia* and *P. aeruginosa* at a MIC of < 4 μg/mL, 6 μg/mL and 6 μg/mL, respectively. All the results obtained were compared with the positive control, ciprofloxacin < 2 μg/mL (Table 2).

3.4. In vivo wound healing

Contraction of the wound area in each group was determined by using grid technique on day 0, 7, 14 and 21 (Fig. 6a and 6b). Significantly ($p < 0.001$) rapid wound contraction was noticed in the LGA composite scaffolds treated group compared to those in control and composite scaffold treated groups. The mean wound area (mm^2) reduction in LGA composite scaffolds treated group was found to be significantly (1.10 ± 0.1 0 mm^2 on day 21, $p < 0.001$) faster in comparison with those in control (51.33 ± 0.82 mm^2 on day 21, $p < 0.01$) and composite scaffolds ($11.79 \pm 1.4\%$ on day 21, $p < 0.01$).

Diabetes causes multifactorial symptoms that include biochemical, vascular, neuropathic, immune function abnormalities that delay the wounds' healing process (Sanapalli et al., 2019). To mimic the human condition in rats, high dose of STZ was used intraperitoneally followed by feeding the rodents with high fat diet, which ultimately results in selective damage of the pancreatic β-cells. This primes to inhibition of synthesis and insulin release, leading to type 2 diabetes after 2 to 3 days (Brem and Tomic-Canic, 2007; Tsuboi et al., 1992).

Open wounds were created in the diabetic rats and the treatment was done for 21 days. Reduction in the mean wound area was calculated for all the groups on day 0, 7, 14 and 21. Rats treated with the LGA composite scaffold showed a varying degree of wound contraction when compared with composite scaffold and untreated groups. The initial inflammatory responses to injury provide the necessary framework for the subsequent production of a new functional barrier The next stage of wound healing is the proliferative phase, which lasts for 3–14 days. More than 60% of the reduction in the wound area was observed in the LGA composite scaffold group.

In contrast, the wound's only 52% and 39% reduction were seen in the composite scaffold and control group on day 7, respectively. Contraction of the wound starts once the inflammatory and proliferative phase completes. This depicts that LGA helped suppress the inflammation phase, COL and CS helped in the proliferation and migration of cells, resulting in 99% of wound healing in 21 days.

3.5. Hydroxyproline estimation

The hydroxyproline content of skin samples after surgery is depicted in Fig. 7. Hydroxyproline content was found to be higher in the LGA composite scaffolds treated group when compared with those in the control group. Although the hydroxyproline content of the composite scaffold treated group was marginally higher than in the control group, the levels were not very significant. The estimation of hydroxyproline levels is an indirect measure of COL concentration. COL is the most abundant component of the extracellular matrix, which is required for wound contraction. Collagen production, accumulation, remodelling, and maturation are all important stages in tissue repair and regeneration (Sa and DiPietro, 2010). Collagen synthesis is mostly influenced by the availability of proline. Proline is actively generated from LGA in the granulation tissues. The increased collagen content observed in the LGA composite scaffolds treated group is most likely related to the availability of extracellular glutamic acid (Aalto et al., 1973). The results show that adding LGA probably increased proline production. Hence, the collagen content of the granulation tissues increased.

3.6. Histopathological studies

The histopathological studies revealed that all the wounds were free from oozing after day 7th post-injury (Fig. 8). Cell infiltration in the control group on the day 7th post-treatment was observed along with the neutrophils, intermittent lymphocytes, and macrophages. A smaller number of neutrophils and macrophages were observed in the composite scaffold group treated animals compared to those in control groups. The LGA composite scaffold treated groups have shown a small number of neutrophils and macrophages compared to those in control.

On the day 14th post-treatment, in the control group, neutrophils still present with few multinucleated massive cells and histiocytes. In the composite scaffold treatment groups, a small number of histiocytes and massive multinucleated cells were seen, whereas in the LGA composite scaffolds treated group abundant histiocytes, multinucleated giant cells and single lymphocytes were observed.

On day 21st post-treatment, the leading response of inflammation by neutrophils in the control groups was reduced. However, control groups showed the recurrence of macrophages and histiocytes. The composite scaffold groups showed a moderate numeral of histiocytes and lymphocytes. In contrast, those treated with LGA composite scaffold treated groups were found to be rich in histiocytes, large multinucleated cells, and lymphocytes.

Control wounds showed neutrophils predominantly along with some monocytes and lymphocytes. As stated in the literature, neutrophils are responsible for wound debridement in the early stage of wound healing. However, an excess number of neutrophils is known to negatively influence the wound

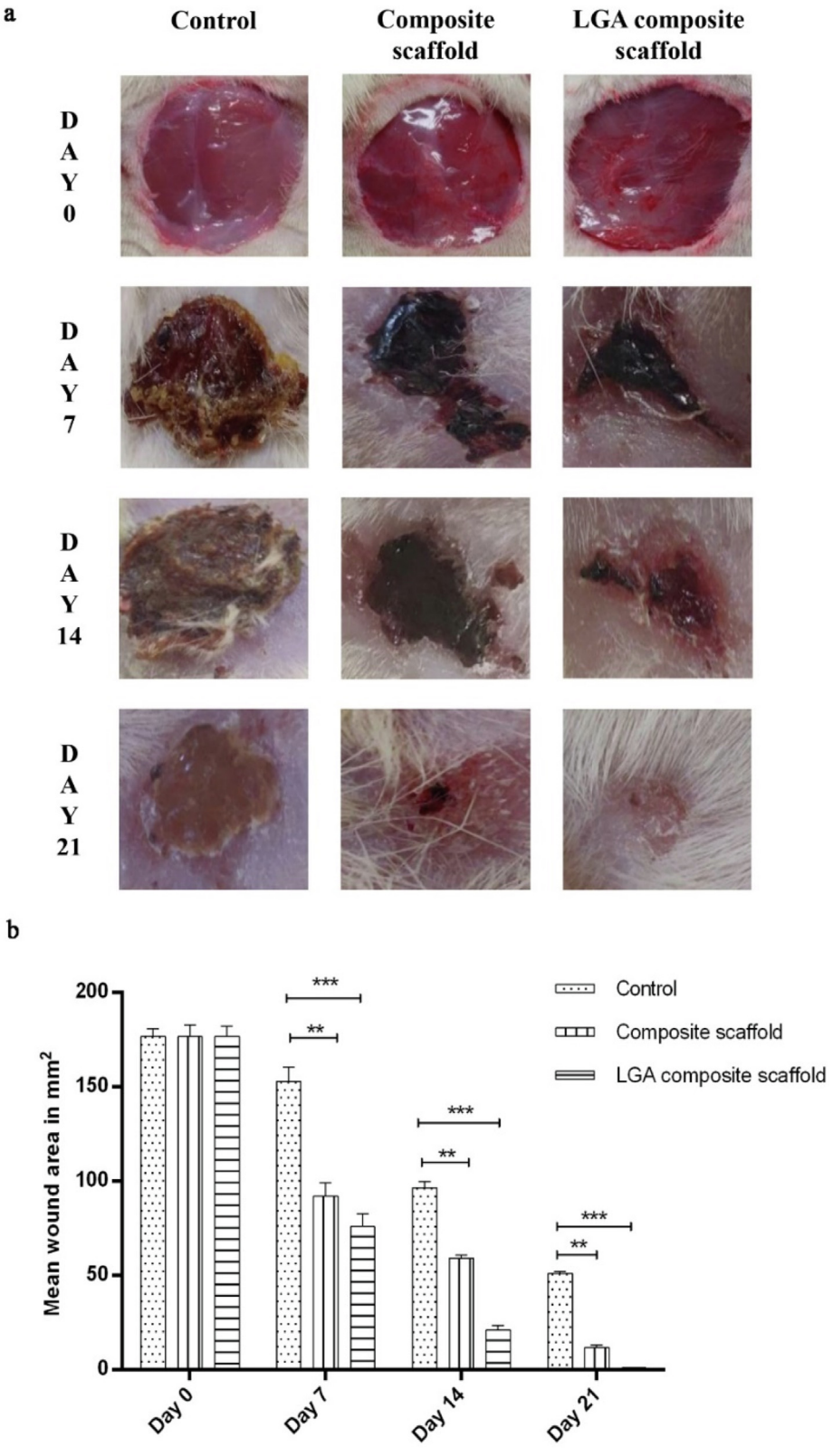

Fig. 6 (a) Images representing the wound contraction in the control, composite scaffold and LGA composite scaffold treated groups from day 0 to 21 post wounding (b) Graphical representation of percentage wound reduction in the control, composite scaffold and LGA composite scaffold treated groups from day 0 to 21 post wounding. Data is expressed as mean ± SD (n = 6 wounds/ group).

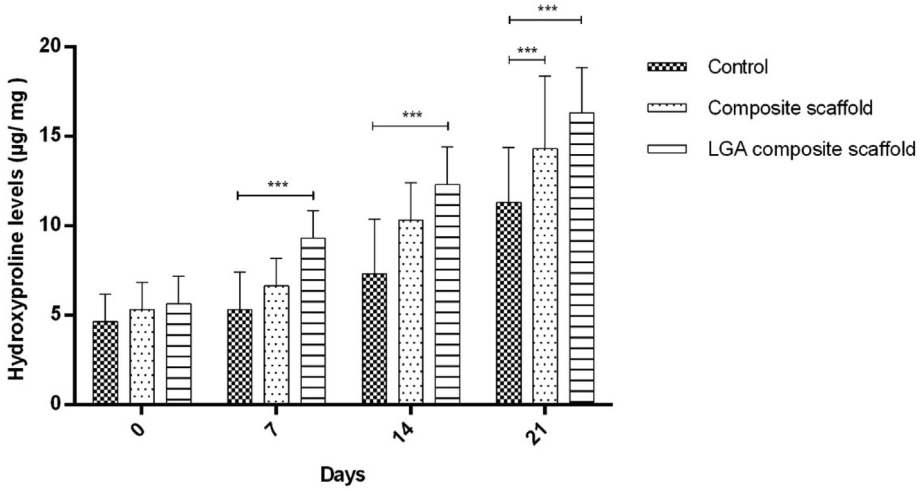

Fig. 7 Result representing the estimation of the hydroxyproline content of wound on day 0, 7, 14 and 21 as an indirect collagen level estimation indicator. The results are represented in µg hydroxyproline/ mg of dry wound tissue. The data represents Mean ± SD (n = 6 wounds/ group). One Way Analysis of Variance (ANOVA) obtained statistical significance, followed by Dunnet's post hoc test.

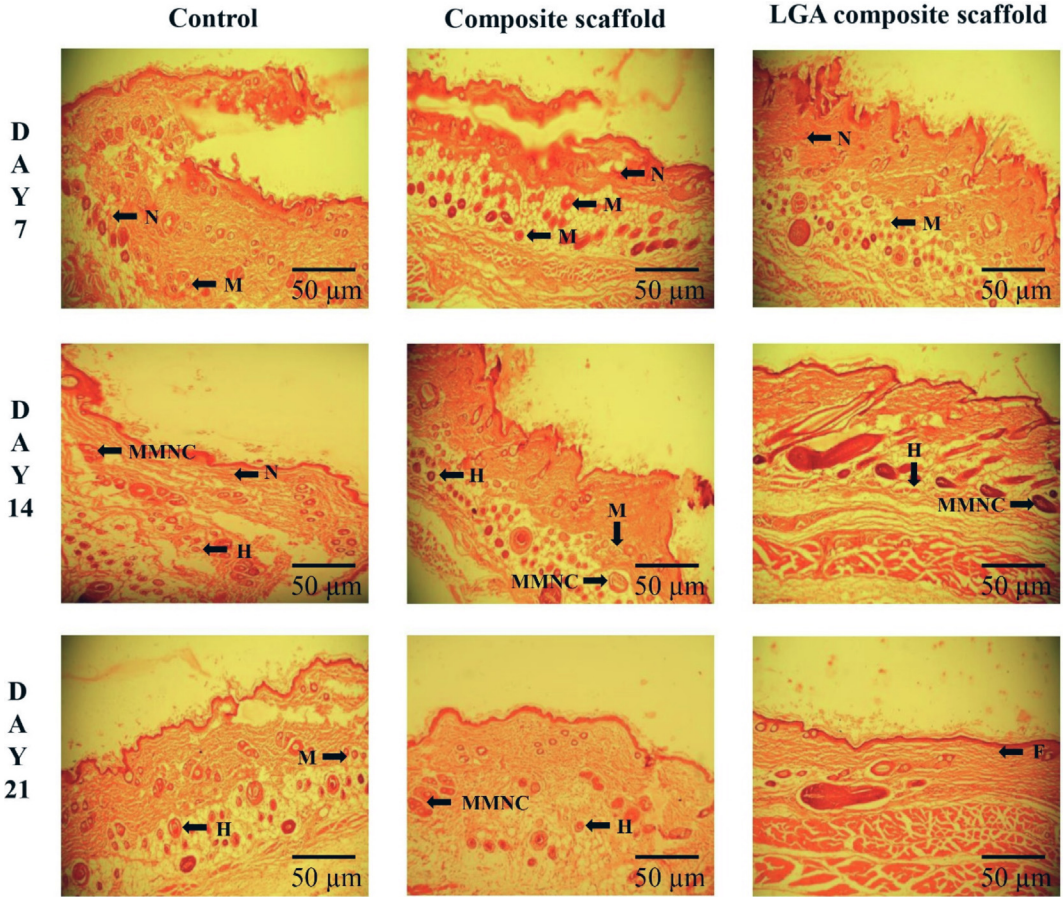

Fig. 8 Histological changes during the wound healing process in STZ induced diabetes wistar albino rat skin on days 7, 14, and 21 without (control) and with treatment (Composite scaffold and LGA composite scaffold) in a full-thickness excision wound model; neutrophils (N), macrophage (M), histiocytes (H), massive multinucleated cell (MMNC), fibroblast (F).

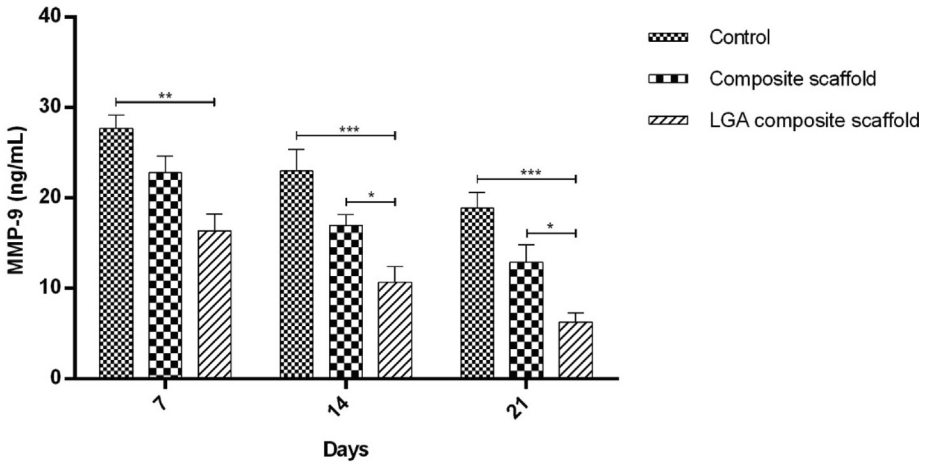

Fig. 9 Graph representing the MMP-9 levels in fluids obtained from healed wounds in STZ induced diabetic rat model on day 21. Levels of MMP-9 were determined in 100-fold aliquots of wound fluids using ELISA analysis. The data represent Mean ± SD (n = 3).

repair and healing process by destroying the normal tissue, as pertinent to previous studies (Dovi et al., 2003).

In the LGA composite scaffold treated group, a higher collection of macrophages and their morphological variants such as multinucleated massive cells and histiocytes were observed. The presence of these cells favors the environment for wound healing. Macrophages have a more important role in repair than defense and promote the COL fiber synthesis that helps in wound closure and healing.

3.7. ELISA test

MMP-9 content in the LGA composite scaffold and composite scaffold treated groups was found to be less in comparison with those in the control group in all days of study. However, MMP-9 content of composite scaffold treated groups was marginally decreased in contrast to those in LGA composite scaffold treated groups (Fig. 9). The significant decrease of MMP-9 in the LGA composite scaffold treated group may be attributed to the anti-inflammatory property of LGA, which prevented the breakdown of formed COL leading to accelerated healing. As noticed earlier, the results of MMP-9 levels in skin homogenates were in good agreement with the visual results recorded for wound contraction (Fig. 6a). The results are in well agreement with the study by Pegorier et al. (2006).

4. Conclusion

The prepared LGA composite scaffold satisfied the prerequisites of an optimum DW dressing in terms of mechanical resilience, swelling, porosity, biodegradation, controlled release, biocompatibility, antibacterial with anti-inflammatory properties that are well-thought-out to be essential for tissue recovery in DWs. Therefore, the current study specifies the combination of LGA as an anti-inflammatory agent, COL as a structural matrix stabilizer, and CS as an antibacterial agent, a potential approach in treating DWs. This combinational strategy of topical application in DW patients might provide a significant clinical outcome.

Availability of data and material

Not applicable.

Code availability

Not applicable.

Funding

This research was supported by the JSS Academy of Higher Education & Research (JSSAHER)-Reg/DIR(R)/URG/54/2011-12/6915.

CRediT authorship contribution statement

Bharat Kumar Reddy Sanapalli: Methodology, Writing: Original Draft, Review and Editing. **Rishita Tyagi:** Methodology. **Afzal B. Shaik:** Writing: Review. **Ranakishor Pelluri:** Formal. **Richie R. Bhandare:** Supervision. **Sivakumar Annadurai:** Supervision. **Veera Venkata Satyanarayana Reddy Karri:** Supervision.

Acknowledgment

The authors would like to thank the Department of Science and Technology – Fund for Improvement of Science and Technology Infrastructure in Universities and Higher Educational Institutions (DST-FIST), New Delhi, for their infrastructure support to our department. The RRB is thankful for Deanship of Graduate Studies and Research, Ajman University for providingfunding towards the APC.

References

International Diabetes Federation. IDF Diabetes Atlas, 8th edn. Brussels, Belgium: International Diabetes Federation, 2017. [Available from: http://www.diabetesatlas.org].

Lipsky, B.A., Berendt, A.R., Deery, H.G., Embil, J.M., Joseph, W.S., Karchmer, A.W., et al, 2004. Diagnosis and treatment of diabetic foot infections. Clin. Infect. Dis. 885–910.

Alexiadou, K., Doupis, J., 2012. Management of diabetic foot ulcers. Diabetes Therapy. 3 (1), 4.

Frykberg, R.G., Banks, J., 2015. Challenges in the treatment of chronic wounds. Advances in wound care. 4 (9), 560–582.

Mat Saad, A.Z., Khoo, T.L., Halim, A.S., 2013. Wound bed preparation for chronic diabetic foot ulcers. ISRN endocrinology. 2013.
Falanga, V., 2005. Wound healing and its impairment in the diabetic foot. The Lancet. 366 (9498), 1736–1743.
Caley, M.P., Martins, V.L., O'Toole, E.A., 2015. Metalloproteinases and wound healing. Advances in wound care. 4 (4), 225–234.
Gill, S.E., Parks, W.C., 2008. Metalloproteinases and their inhibitors: regulators of wound healing. The international journal of biochemistry & cell biology. 40 (6–7), 1334–1347.
Reiss, M.J., Han, Y.-P., Garcia, E., Goldberg, M., Yu, H., Garner, W. L., 2010. Matrix metalloproteinase-9 delays wound healing in a murine wound model. Surgery. 147 (2), 295–302.
Wu, C., Qin, X., Du, H., Li, N., Ren, W., Peng, Y., 2017. The immunological function of GABAergic system. Front Biosci. 22, 1162–1172.
Huang, Q., Liu, C., Wang, C., Hu, Y., Qiu, L., Xu, P., 2011. Neurotransmitter γ-aminobutyric acid-mediated inhibition of the invasive ability of cholangiocarcinoma cells. Oncology letters. 2 (3), 519–523.
Bano, I., Arshad, M., Yasin, T., Ghauri, M.A., Younus, M., 2017. Chitosan: A potential biopolymer for wound management. Int. J. Biol. Macromol. 102, 380–383.
Zhang, D., Zhou, W., Wei, B., Wang, X., Tang, R., Nie, J., et al, 2015. Carboxyl-modified poly (vinyl alcohol)-crosslinked chitosan hydrogel films for potential wound dressing. Carbohydr. Polym. 125, 189–199.
Foroumadi, A., Davood, A., Mirzaei, M., Emami, S., Moshafi, M., 2001. Synthesis and antibacterial activity of some novel N-substituted piperazinyl-quinolones. Boll. Chim. Farm. 140 (6), 411–416.
Deutsch, C., Edwards, D., Myers, S., 2017. Wound dressings. Br. J. Hosp. Med. 78 (7), C103–C109.
O'Meara, S., Cullum, N., Majid, M., Sheldon, T., 2000. Systematic reviews of wound care management:(3) antimicrobial agents for chronic wounds;(4) diabetic foot ulceration. Health technology assessment (Winchester, England). 4 (21), 1–237.
Jayakumar, R., Prabaharan, M., Kumar, P.S., Nair, S., Tamura, H., 2011. Biomaterials based on chitin and chitosan in wound dressing applications. Biotechnol. Adv. 29 (3), 322–337.
Xiao, B., Wan, Y., Zhao, M., Liu, Y., Zhang, S., 2011. Preparation and characterization of antimicrobial chitosan-N-arginine with different degrees of substitution. Carbohydr. Polym. 83 (1), 144–150.
Nair, L.S., Laurencin, C.T., 2005. Polymers as biomaterials for tissue engineering and controlled drug delivery. Springer, Tissue engineering I, pp. 47–90.
Ulery, B.D., Nair, L.S., Laurencin, C.T., 2011. Biomedical applications of biodegradable polymers. J. Polym. Sci., Part B: Polym. Phys. 49 (12), 832–864.
Vinatier, C., Mrugala, D., Jorgensen, C., Guicheux, J., Noël, D., 2009. Cartilage engineering: a crucial combination of cells, biomaterials and biofactors. Trends Biotechnol. 27 (5), 307–314.
Morrison, W.A., 2009. Progress in tissue engineering of soft tissue and organs. Surgery. 145 (2), 127–130.
Gautam, S., Dinda, A.K., Mishra, N.C., 2013. Fabrication and characterization of PCL/gelatin composite nanofibrous scaffold for tissue engineering applications by electrospinning method. Mater. Sci. Eng., C 33 (3), 1228–1235.
Jafari, M., Paknejad, Z., Rad, M.R., Motamedian, S.R., Eghbal, M.J., Nadjmi, N., et al, 2017. Polymeric scaffolds in tissue engineering: a literature review. J. Biomed. Mater. Res. B Appl. Biomater. 105 (2), 431–459.
Ricard-Blum, S., 2011. The collagen family. Cold Spring Harbor Perspect. Biol. 3, (1) a004978.
Inzana, J.A., Olvera, D., Fuller, S.M., Kelly, J.P., Graeve, O.A., Schwarz, E.M., et al, 2014. 3D printing of composite calcium phosphate and collagen scaffolds for bone regeneration. Biomaterials 35 (13), 4026–4034.
Lu, C., Meng, D., Cao, J., Xiao, Z., Cui, Y., Fan, J., et al, 2015. Collagen scaffolds combined with collagen-binding ciliary neurotrophic factor facilitate facial nerve repair in mini-pigs. J. Biomed. Mater. Res. Part A 103 (5), 1669–1676.
Ghazanfari, S., Driessen-Mol, A., Strijkers, G.J., Baaijens, F.P., Bouten, C.V., 2015. The evolution of collagen fiber orientation in engineered cardiovascular tissues visualized by diffusion tensor imaging. PLoS ONE 10, (5) e0127847.
Meimandi-Parizi, A., Oryan, A., Moshiri, A., 2013. Role of tissue engineered collagen based tridimensional implant on the healing response of the experimentally induced large Achilles tendon defect model in rabbits: a long term study with high clinical relevance. J. Biomed. Sci. 20 (1), 28.
Gelse, K., Pöschl, E., Aigner, T., 2003. Collagens—structure, function, and biosynthesis. Adv. Drug Deliv. Rev. 55 (12), 1531–1546.
Chevallay, B., Herbage, D., 2000. Collagen-based biomaterials as 3D scaffold for cell cultures: applications for tissue engineering and gene therapy. Med. Biol. Eng. Compu. 38 (2), 211–218.
Wolf K, Alexander S, Schacht V, Coussens LM, von Andrian UH, van Rheenen J, et al., editors. Collagen-based cell migration models in vitro and in vivo. Seminars in cell & developmental biology; 2009: Elsevier.
Wang, W., Zhang, Y., Ye, R., Ni, Y., 2015. Physical crosslinkings of edible collagen casing. Int. J. Biol. Macromol. 81, 920–925.
Takitoh, T., Bessho, M., Hirose, M., Ohgushi, H., Mori, H., Hara, M., 2015. Gamma-cross-linked nonfibrillar collagen gel as a scaffold for osteogenic differentiation of mesenchymal stem cells. J. Biosci. Bioeng. 119 (2), 217–225.
Maslennikova, A., Kochueva, M., Ignatieva, N., Vitkin, A., Zakharkina, O., Kamensky, V., et al, 2015. Effects of gamma irradiation on collagen damage and remodeling. Int. J. Radiat Biol. 91 (3), 240–247.
Gordon, M.K., Hahn, R.A., 2010. Collagens. Cell and tissue research. 339 (1), 247.
Balan, V., Verestiuc, L., 2014. Strategies to improve chitosan hemocompatibility: A review. Eur. Polym. J. 53, 171–188.
Ueno, H., Nakamura, F., Murakami, M., Okumura, M., Kadosawa, T., Fujinaga, T., 2001. Evaluation effects of chitosan for the extracellular matrix production by fibroblasts and the growth factors production by macrophages. Biomaterials 22 (15), 2125–2130.
Patrulea, V., Ostafe, V., Borchard, G., Jordan, O., 2015. Chitosan as a starting material for wound healing applications. Eur. J. Pharm. Biopharm. 97, 417–426.
Dragostin, O.M., Samal, S.K., Dash, M., Lupascu, F., Pânzariu, A., Tuchilus, C., et al, 2016. New antimicrobial chitosan derivatives for wound dressing applications. Carbohydr. Polym. 141, 28–40.
He, Q., Ao, Q., Gong, Y., Zhang, X., 2011. Preparation of chitosan films using different neutralizing solutions to improve endothelial cell compatibility. J. Mater. Sci. - Mater. Med. 22 (12), 2791–2802.
Anisha, B., Sankar, D., Mohandas, A., Chennazhi, K., Nair, S.V., Jayakumar, R., 2013. Chitosan–hyaluronan/nano chondroitin sulfate ternary composite sponges for medical use. Carbohydr. Polym. 92 (2), 1470–1476.
Dutta, P., Rinki, K., Dutta, J., 2011. Chitosan: A promising biomaterial for tissue engineering scaffolds. Springer, Chitosan for biomaterials II, pp. 45–79.
Ammar, H., Ghorab, M., El-Nahhas, S., Kamel, R., 2009. Polymeric matrix system for prolonged delivery of tramadol hydrochloride, part I: physicochemical evaluation. Aaps Pharmscitech. 10 (1), 7–20.
Kamel, R., 2013. Study of the influence of selected variables on the preparation of prolonged release bioadhesive vaginal carbohydrate microspheres using experimental design. J. Drug Delivery Sci. Technol. 23 (3), 247–254.

Kamel, R., Abbas, H., 2018. A multi-microcarrier of metronidazole-biopolymers complexes as a potential vaginal delivery system. International Journal of Polymeric Materials and Polymeric Biomaterials. 67 (4), 239–246.
Ureña-Saborio, H., Alfaro-Viquez, E., Esquivel-Alvarado, D., Esquivel, M., Madrigal-Carballo, S., 2018. Collagen/chitosan hybrid 3D-scaffolds as potential biomaterials for tissue engineering. Int. J. Nano Biomater. 7 (3), 163–175.
Natarajan, J., Sanapalli, B.K.R., Bano, M., Singh, S.K., Gulati, M., Karri, V.V.S.R., 2019. Nanostructured Lipid Carriers of Pioglitazone Loaded Collagen/Chitosan Composite Scaffold for Diabetic Wound Healing. Advances in Wound Care.
Karri, V.V.S.R., Kuppusamy, G., Talluri, S.V., Mannemala, S.S., Kollipara, R., Wadhwani, A.D., et al, 2016. Curcumin loaded chitosan nanoparticles impregnated into collagen-alginate scaffolds for diabetic wound healing. Int. J. Biol. Macromol. 93, 1519–1529.
Powell, H.M., Boyce, S.T., 2006. EDC cross-linking improves skin substitute strength and stability. Biomaterials 27 (34), 5821–5827.
Baheiraei, N., Nourani, M.R., Mortazavi, S.M.J., Movahedin, M., Eyni, H., Bagheri, F., et al, 2018. Development of a bioactive porous collagen/β-tricalcium phosphate bone graft assisting rapid vascularization for bone tissue engineering applications. J. Biomed. Mater. Res. Part A 106 (1), 73–85.
Kim, Y., Kim, G., 2013. Collagen/alginate scaffolds comprising core (PCL)–shell (collagen/alginate) struts for hard tissue regeneration: fabrication, characterisation, and cellular activities. J. Mater. Chem. B 1 (25), 3185–3194.
Xie, Y., Chen, J., Xiao, A., Liu, L., 2017. Antibacterial activity of polyphenols: structure-activity relationship and influence of hyperglycemic condition. Molecules 22 (11), 1913.
Geerlings, S.E., Brouwer, E.C., Gaastra, W., Verhoef, J., Hoepelman, A.I., 1999. Effect of glucose and pH on uropathogenic and non-uropathogenic Escherichia coli: studies with urine from diabetic and non-diabetic individuals. J. Med. Microbiol. 48 (6), 535–539.
Eloff, J.N., 1998. A sensitive and quick microplate method to determine the minimal inhibitory concentration of plant extracts for bacteria. Planta Med. 64 (08), 711–713.
Zhang, M., Lv, X.-Y., Li, J., Xu, Z.-G., Chen, L., 2009. The characterization of high-fat diet and multiple low-dose streptozotocin induced type 2 diabetes rat model. Experimental diabetes research. 2008.
Sanapalli, B.K.R., Kannan, E., Balasubramanian, S., Natarajan, J., Baruah, U.K., Karri, V.V.S.R., 2018. Pluronic lecithin organogel of 5-aminosalicylic acid for wound healing. Drug Dev. Ind. Pharm. 44 (10), 1650–1658.
Reddy, G.K., Enwemeka, C.S., 1996. A simplified method for the analysis of hydroxyproline in biological tissues. Clin. Biochem. 29 (3), 225–229.
Wang, X., Li, D., Wang, W., Feng, Q., Cui, F., Xu, Y., et al, 2003. Crosslinked collagen/chitosan matrix for artificial livers. Biomaterials 24 (19), 3213–3220.
Kołodziejska, I., Piotrowska, B., Bulge, M., Tylingo, R., 2006. Effect of transglutaminase and 1-ethyl-3-(3-dimethylaminopropyl) carbodiimide on the solubility of fish gelatin–chitosan films. Carbohydr. Polym. 65 (4), 404–409.
Mane, S., Ponrathnam, S., Chavan, N., 2015. Effect of chemical cross-linking on properties of polymer microbeads: A review. Can Chem Trans. 3 (4), 473–485.
Ma, L., Gao, C., Mao, Z., Zhou, J., Shen, J., Hu, X., et al, 2003. Collagen/chitosan porous scaffolds with improved biostability for skin tissue engineering. Biomaterials 24 (26), 4833–4841.
Rehakova M, Bakoš D, Vizarova K, Soldán M, Juríč ková M. Properties of collagen and hyaluronic acid composite materials and their modification by chemical crosslinking. Journal of Biomedical Materials Research: An Official Journal of The Society for Biomaterials and The Japanese Society for Biomaterials. 1996;30 (3):369-72.
Haugh, M.G., Murphy, C.M., McKiernan, R.C., Altenbuchner, C., O'Brien, F.J., 2011. Crosslinking and mechanical properties significantly influence cell attachment, proliferation, and migration within collagen glycosaminoglycan scaffolds. Tissue Eng. Part A 17 (9–10), 1201–1208.
Timmer, M.D., Ambrose, C.G., Mikos, A.G., 2003. In vitro degradation of polymeric networks of poly (propylene fumarate) and the crosslinking macromer poly (propylene fumarate)-diacrylate. Biomaterials 24 (4), 571–577.
Pillay, V., Fassihi, R., 1999. In vitro release modulation from crosslinked pellets for site-specific drug delivery to the gastrointestinal tract: I. Comparison of pH-responsive drug release and associated kinetics. J. Control. Release 59 (2), 229–242.
Sailakshmi, G., Mitra, T., Gnanamani, A., 2013. Engineering of chitosan and collagen macromolecules using sebacic acid for clinical applications. Prog. Biomater. 2 (1), 11.
Thangavel, P., Ramachandran, B., Chakraborty, S., Kannan, R., Lonchin, S., Muthuvijayan, V., 2017. Accelerated healing of diabetic wounds treated with L-glutamic acid loaded hydrogels through enhanced collagen deposition and angiogenesis: an in vivo study. Scientific reports. 7 (1), 1–15.
Sanapalli, B.K., Yele, V., Kalidhindi, R.S., Singh, S.K., Gulati, M., Karri, V.V., 2019. Human beta defensins may be a multifactorial modulator in the management of diabetic wound. Wound Repair and Regeneration.
Brem, H., Tomic-Canic, M., 2007. Cellular and molecular basis of wound healing in diabetics J Clin Invest. 117, 1219–1222.
Tsuboi, R., Shi, C.M., Rifkin, D.B., Ogawa, H., 1992. A wound healing model using healing-impaired diabetic mice. The Journal of dermatology. 19 (11), 673–675.
Sa, G., DiPietro, L.A., 2010. Factors affecting wound healing. J. Dent. Res. 89 (3), 219–229.
Aalto, M., Lampiaho, K., Pikkarainen, J., Kulonen, E., 1973. Amino acid metabolism of experimental granulation tissue in vitro. Biochem. J 132 (4), 663–671.
Dovi, J.V., He, L.K., DiPietro, L.A., 2003. Accelerated wound closure in neutrophil-depleted mice. J. Leukoc. Biol. 73 (4), 448–455.
Pégorier, S., Wagner, L.A., Gleich, G.J., Pretolani, M., 2006. Eosinophil-derived cationic proteins activate the synthesis of remodeling factors by airway epithelial cells. J. Immunol. 177 (7), 4861–4869.